MULTISCALE IMAGE ANALYSIS BASED ON ROBUST AND ADAPTIVE MORPHOLOGICAL SCALE-SPACES

El Hadji Samba Diop, Jesus Angulo

MULTISCALE IMAGE ANALYSIS BASED ON ROBUST AND ADAPTIVE MORPHOLOGICAL SCALE-SPACES

by

El Hadji S. Diop[a] and Jesús Angulo

Center of Mathematical Morphology, Department of Mathematics and Systems, MINES ParisTech, 35 rue Saint-Honor, 77305 Fontainebleau Cedex - France

E-mail: ehsdiop@hotmail.com, jesus.angulo@mines-paristech.fr

Abbreviated running title: Robust and Adaptive Scale-Spaces

Abbreviated authors: Diop E.H.S. and Angulo J.

Key words: Partial differential equations. Morphological operators. Robustness. Adaptability

---

[a]Actually within the Departement of Mathematics, University of Thies, Cité Malick SY, BP 967, Thiès, Sénégal

ABSTRACT

Mathematical morphology is a powerful tool for image analysis; however, classical morphological operators suffer from lacks of robustness against noise, and also intrinsic image features are not accounted at all in the process. We propose in this work a new and different way to overcome such limits, by introducing both robustness and locally adaptability in morphological operators, which are now defined in a manner such that intrinsic image features are accounted. Dealing with partial differential equations (PDEs) for generalized Cauchy problems, we show that proposed PDEs are equivalent to impose robustness and adaptability of corresponding sup-inf operators, to structuring functions. Accurate numerical schemes are also provided to solve proposed PDEs, and experiments conducted for both synthetic and real images, show the efficiency and robustness of our approach.

INTRODUCTION

In many image processing and computer vision tasks (*e.g.* data compression, feature detection, motion analysis/detection, multiband frequency analysis, ...), it is important to perform a multiscale image analysis, *i.e.* analyze the image at multiple spatial scales or resolutions. Owing to that fact, mathematical morphology (Serra, 1982) appeared as a powerful tool in multiscale analysis (Soille, 1999), mainly due to its nonlinearity aspects, shape and geometry description properties. Despite its interesting properties and plentiful successful applications in various domains, both former discrete and continuous morphological operators suffer from a lack of robustness against noise, and do not take into account the spatial adaptability. The same global way in which all image pixels are treated is in fact main reasons for that limitations. This is avoided in (Lerallut *et al.*, 2007) by using morphological filters with non fixed shape kernels (or amoebas), and in (Angulo, 2011) by considering bilateral structuring functions. Using a PDE approach, in order to enhance coherence of flow-like structures, an adaptive method was obtained in (Breuβ *et al.*, 2007) by multiplying the image gradient term that appeared in classical morphological PDEs for dilations / erosions, with a space-variant matrix.

Motivation and goal   The main motivation of this work is to propose alternatives for remedying such weaknesses of robustness and adaptability. This is done by considering Perona and Malik-like diffusivity term (Perona and Malik, 1990). Let us first recall some fundamentals of this nonlinear image diffusion model. The pioneering idea introduced by Perona and Malik (Perona and Malik, 1990) to reduce blurring and edge shifting of uniform linear diffusion, involved a locally adaptive diffusion with respect to the gradient of the image at each iteration. More precisely, this nonlinear diffusion involves replacing the heat transfer diffusion equation $\frac{\partial u}{\partial t} = \Delta u$, by the following model:

$$\begin{cases} \dfrac{\partial u}{\partial t} = \text{div}\left(g\left(\|\nabla u\|^2\right)\nabla u\right) \\ u(x,0) = f(x). \end{cases} \tag{1}$$

In this model (1), the diffusivity has to be such that $g\left(\|\nabla u\|^2\right) \to 0$ when $\|\nabla u\|^2 \to \infty$, and $g\left(\|\nabla u\|^2\right) \to 1$ when $\|\nabla u\|^2 \to 0$. One of the diffusivities proposed by Perona and Malik is the following:

$$g(s^2) = 1 / \left(1 + (s^2/\lambda^2)\right), \, \lambda > 0,$$

where λ is a threshold parameter that separates forward and backward diffusion. This model accomplishes the aim of blurring small fluctuations (noise) while enhancing edges (by preventing excessive diffusion). To avoid theoretical as well as numerical drawbacks on this model, Catt et *al.* proposed (Catté *et al.*, 1992) a new version of Perona and Malik theory, by replacing the diffusivity term $g\left(\|\nabla u\|^2\right)$ with its regularized version, *i.e.* $g\left(\|\nabla u_\sigma\|^2\right)$ where $\nabla u_\sigma = \nabla\left(G_\sigma * u\right)$, and G_σ is a Gaussian kernel with a standard deviation equal to σ. This latter model is nowadays extremely popular in PDE-based image processing, and many variants have then been proposed.

Concretely, we wish in this work to meet two major objectives. On a first hand, we aim at exploring how a gradient-based local adaptability such as $g\left(\|\nabla u\|^2\right)$, can be introduced in both morphological PDEs and sup-inf based operators. On a second hand, we would like to propose associated numerical schemes for solving efficiently proposed methods.

State-of-the art on discrete adaptive morphology Original formulation of discrete dilation and erosion for gray-level images (Serra, 1982; Sternberg, 1986), as well as the other morphological operators was translation invariant in space and intensity. Later, mathematical morphology was formulated in the framework of complete lattices (Serra, 1988; Heijmans and Ronse, 1990), which leads to a general case of dilation and adjoint erosion compatible with spatially-variant operators. Nevertheless, most of current implementations and classical applications studied in the literature are based on morphological operators, which are translation invariant in space and intensity (Soille, 1999), *i.e.* a same structuring function (or structuring element) is considered for each pixel of the image. A current active field in mathematical morphology is the construction of appropriate

adaptive operators; *i.e.* structuring functions become dependent on the position or on the input image itself. In previous works, adaptive operators are based on two main approaches. On a first hand, a variability is considered on the support space of pixels, meaning that spatially variable shape of structuring functions are adapted according to:

(i)   positions in the image, as in (Beucher *et al.*, 1987; Cuisenaire, 2006)

(ii)   local regularity including the morphological amoebas (Lerallut *et al.*, 2007), adaptive geodesic neighborhoods (Grazzini and Soille, 2009), bilateral structuring function (Angulo, 2011)

(iii)   local orientations, including typically anisotropic gradient-driven operators (Verdú-Monedero *et al.*, 2011).

On another hand, a variability on $\mathscr{T}$ is considered: variable size of structuring functions according to the local intensity or contrast (Vachier and Meyer, 2007; Maragos and Vachier, 2008).

For an overview on the state-the-art on adaptive morphology, the interested reader is invited to the paper (Maragos and Vachier, 2009). Another recent study (Roerdink, 2009) is very interesting for understanding the theoretical limitations of input-adaptive morphological operators.

State-of-the art on PDEs-based morphological operators   In 1992, three independent milestones papers appeared on nonlinear PDEs for modeling continuous multiscale morphological operators:

–   In (Alvarez *et al.*, 1992; 1993), authors obtained PDEs for multiscale flat dilations and erosions, by means of compact convex structuring sets as part of their general work on developing PDE-based models for multiscale image processing that satisfy certain axiomatic principles.

- Authors in (Brockett and Maragos, 1992; 1994) developed nonlinear PDEs that model multiscale morphological dilation/erosion, opening/closing, by using compact support structuring elements that are either convex sets or concave functions and may have non smooth boundaries. Appropriate numerical schema were provided as well.

- PDEs for multiscale dilation and erosion were obtained (van den Boomgaard and Smeulders, 1992; 1994) in by studying the propagation of $2D$ boundaries sets and signal graphs, under multiscale dilations and erosions. Their work applies to convex structuring elements whose boundaries contain no linear segments, are smooth, and possess a unique normal at each point.

Paper contributions We provide herein a new approach to make classical multiscale dilation and erosion operators, robust and spatially adaptive as regards to intrinsic image features. To constraint both continuous and sup-inf based models to meet our target objectives, we choose to investigate PDEs forgeneralized Cauchy problems. Parameters of such models are then linked to image features in two ways; the last one being extremely robust in a noisy environment. Moreover, suitable numerical schemes are provided for solving efficiently proposed PDE-based models.

Manuscript organization The paper is organized as follows. We recall in the next section some background on mathematical morphology. After that, we present our proposed robust and adaptive multiscale approach in another section. Afterwards, numerical schemes for solving proposed models are described, and obtained results are shown. The paper ends with some discussions and outline of some interesting perspectives.

BACKGROUND ON MATHEMATICAL MORPHOLOGY

Algebraic lattice theory From a theoretical viewpoint, mathematical morphology is nowadays formulated in the algebraic framework complete lattice theory (Serra, 1988;

Heijmans, 1994). More precisely, the notion of adjunction links two operators (ε, δ), in such a way that for any given dilation δ, there is a unique erosion ε such that (ε, δ) is an adjunction (Heijmans and Ronse, 1990). In this paper, we adopt the alternative paradigm based on functional analysis, which leads to the formulation of dilation and erosion as the solution of PDEs.

Basic morphological operators Since its introduction, mathematical morphology (Matheron, 1975; Serra, 1982) appeared as a powerful tool in image analysis (Soille, 1999). This is mainly due to its nonlinearity, shape and geometry description properties. Let $\mathbb{E} \subseteq \mathbb{Z}^2$. For any function $f : \mathbb{E} \to \bar{\mathbb{R}}$, elementary *dilation* and *erosion* operators (obtained by adjunction and duality) are respectively defined by:

$$(f \oplus b)(x) := \bigvee_{y \in \mathbb{E}} [f(y) + b(x - y)] \tag{2}$$

$$(f \ominus b)(x) := \bigwedge_{y \in \mathbb{E}} [f(y) - b(y - x)], \tag{3}$$

where $\bigvee$ (*resp.* $\bigwedge$) represents the supremum (*resp.* infimum). The further convention for scalar addition in is considered: $f(y) + b(x - y) = -\infty$ when $b(x - y) = -\infty$ or $f(y) = -\infty$, and that $f(y) - b(y - x) = +\infty$ when $b(y + x) = +\infty$ or $f(y) = -\infty$. We notice that dilation and erosion are related respectively to the supremal and infimal convolution known in convex analysis (Rockafellar, 1970). The structuring function $b : \mathbb{R}^2 \to \bar{\mathbb{R}}$ is a general concave function. A simple case of flat dilation and erosion results when b equals to 0 in a convex bounded set $B \subseteq \mathbb{E}$ called structuring element and $-\infty$ outside, *i.e.* $b(x) = 0$ if $x \in B$ and $b(x) = -\infty$ if $x \in B^c$:

$$(f \oplus B)(x) = \bigvee_{y \in B} [f(x - y)] \text{ and } (f \ominus B)(x) = \bigwedge_{y \in B} [f(x + y)].$$

Both dilation and erosion are invariant under translations in $\mathbb{E}$ (spatial or "horizontal" direction) and $\bar{\mathbb{R}}$ (intensity or "vertical" direction).

Definition 2.1 *Let $\mathscr{F}$ be a family of real functions mapped on $\mathbb{E} \subseteq \mathbb{R}^2$. An operator*

$S : \mathscr{F} \to \mathscr{F}$ *is increasing or monotone if for all* $f, g \in \mathscr{F}$ *s.t.* $f(x) \geq g(x)$, $\forall x \in \mathbb{E}$, *then,* $(Sf)(x) \geq (Sg)(x)$, $\forall x \in \mathbb{E}$.

In addition to that, *dilation* and *erosion* are increasing operators, and also satisfy the following properties:

– Duality: $(f \oplus b)(x) = -(-f \ominus b)(x)$, $\forall x \in \mathbb{E}$

– Adjunction: $(f \oplus b)(x) \leq g(x)$, $\forall x \in \mathbb{E} \Longleftrightarrow f(x) \leq (g \ominus b)(x)$, $\forall x \in \mathbb{E}$

Different morphological filters can be obtained by combining above operators (Matheron, 1975; Serra, 1982; Catté *et al.*, 1995; Cao, 1998). Using a concave structuring function b, two interesting operators, namely the *opening* and *closing*, can be obtained respectively in the following way:

$$(f \circ b) := [(f \ominus b) \oplus b] \tag{4}$$

$$(f \bullet b) := [(f \oplus b) \ominus b]. \tag{5}$$

Opening and *closing* are also increasing operators with two main properties:

– Anti-extensivity: $(f \circ b) \leq f \leq (f \bullet b)$

– Idempotence: for any concave structuring function, one has: $[(f \circ b) \circ b] = (f \circ b)$. By duality, one also has: $[(f \bullet b) \bullet b] = (f \bullet b)$

Semi-group property, multiscale morphological filters and morphological PDEs
For $t \geq 0$, one can define then multiscale dilations (and erosions) by replacing b by the family of multiscale structuring functions $(b_t)_{t \geq 0}$ defined for $t > 0$ by:

$$b_t(x) = \begin{cases} tb(x/t) & \text{for } t > 0 \\ 0 & \text{for } t = 0, \ x = 0 \\ -\infty & \text{otherwise,} \end{cases}$$

which satisfies the semi-group property $(b_s \oplus b_t)(x) = b_{s+t}(x,y)$. The canonical multiscale structuring function, which can be seen as the morphological counterpart of the Gaussian kernel in linear filtering, is the infinity support parabolic structuring function

$$b_t(x) = -\frac{\|x\|^2}{2t}.$$

From the works by Van den Boomgaard (van den Boomgaard and Dorst, 1997), it is also well known that this structuring functions are the equivalent class of functions which are dimensionally separable and closed with respect to the dilation/erosion. This result is usually proved in the slope transform domain (Dorst and van den Boomgaard, 1994; Maragos, 1995). Multiscale dilation and erosion filters are then respectively given by:

$$(f \oplus b_t)(x) := \bigvee_{y \in \mathbb{E}} [f(y) + b_t(x-y)] \tag{6}$$

$$(f \ominus b_t)(x) := \bigwedge_{y \in \mathbb{E}} [f(y) - b_t(y-x)]. \tag{7}$$

Let us mention that in the case of flat structuring functions, this is equivalent to consider sets $B_t = tB$ (*i.e.* homothetic compact convex planar sets B of size t) as multiscale structuring elements.

Note that multiscale openings and closings can be defined in a same way by considering a family $(b_t)_{t \geq 0}$ of multiscale structuring functions, respectively by:

$$(f \circ b_t) := [(f \ominus b_t) \oplus b_t] \tag{8}$$

$$(f \bullet b_t) := [(f \oplus b_t) \ominus b_t]. \tag{9}$$

Alternatives to perform multiscale continuous flat dilations and erosions (dual operators) by using partial differential equations (PDEs) were proposed in (Alvarez *et al.*, 1993; Sapiro *et al.*, 1993; Brockett and Maragos, 1994):

$$\begin{cases} \dfrac{\partial u}{\partial t} = \pm \|\nabla u\| \\ u(x,0) = f(x). \end{cases} \tag{10}$$

with $(+)$ (*resp.* $(-)$) sign in (10) stands for the multiscale dilation (*resp.* erosion). Useful cases of unit structuring sets B are obtained by unit balls $B|_p = \{x \in \mathbb{R}^n : \|x\|_p \leq 1\}$ of metrics induced by the L_p norms. There are three special cases of norms $p = 1, 2$ and $p = \infty$ which correspond to particular PDEs: for $B|_1$ (*i.e.* rhombus), one has $\partial u_t = \pm\|\nabla u\|_\infty$; for $B|_2$ (*i.e.* disk), one has $\partial u_t = \pm\|\nabla u\|_2$; and for $B|_\infty$ (*i.e.* square), one has $\partial u_t = \pm\|\nabla u\|_1$. Similarly, the PDE for multiscale parabolic dilations and erosions is given by:

$$\begin{cases} \dfrac{\partial u}{\partial t} = \pm\dfrac{1}{2}\|\nabla u\|^2 \\ u(x, 0) = f(x). \end{cases} \tag{11}$$

It is well known that both dilation/erosion PDEs (10) and (11) are special cases of Hamilton-Jacobi equations, which are of great interests in physics. In fact, let us consider the general Hamilton-Jacobi equations:

$$\begin{cases} \dfrac{\partial u(x,t)}{\partial t} = \pm H\left(x, \nabla u(x,t)\right) = 0 \text{ in } \mathbb{R}^n \times (0, +\infty) \\ u(\cdot, 0) = f \text{ in } \mathbb{R}^n. \end{cases} \tag{12}$$

Such equations usually do not admit classic (*i.e.* everywhere differentiable) solutions, but they can be studied in the framework of viscosity solutions theory (Crandall *et al.*, 1992). It is well known (Lions, 1982; Bardi and Evans, 1984) that if the Hamiltonian $H(x, p) = H(p)$ is convex, then, the solution of the Cauchy problem are respectively given for the $(+)$ and $(-)$ signs in (12), by:

$$u(x, t) = \inf_{y \in \mathbb{R}^n}\left[f(y) + tH^*\left(\frac{x - y}{t}\right)\right] \tag{13}$$

$$u(x, t) = \sup_{y \in \mathbb{R}^n}\left[f(y) - tH^*\left(\frac{x - y}{t}\right)\right], \tag{14}$$

where H^* is the Legendre-Fenchel transform of function H.

Finally, let us quote works in (Alvarez *et al.*, 1993) in which authors proposed the

following PDE for multiscale continuous openings, given for any scale $s > 0$ by:

$$\begin{cases} \dfrac{\partial u}{\partial t} = -\text{sign}^+(s-t)\|\nabla u\| + \text{sign}^+(t-s)\|\nabla u\| \\ u(x,0) = f(x), \end{cases} \tag{15}$$

with $t \in [0, 2s]$; $\text{sign}(\cdot)$ stands for the signum function and $r^+ := \max(r,0)$. Indeed, for $t \in [0, s]$, PDE (15) acts as a multiscale erosion, while for $t \in]s, 2s]$ it is in fact a multiscale dilation. Multiscale closings can be obtained by switching $(+)$ and $(-)$ signs in the two terms of PDE (15).

PROPOSED ROBUST AND SPATIALLY ADAPTIVE SCALE-SPACES

It is clear that neither the discrete (*cf.* equations (2) and (3)) nor the continuous (10) formulations are robust in a noisy environment. In fact, in the presence of noise, taking the supremum (2) or the infimum (3) will definitely lead to wrong values, while hyperbolic PDEs (10) will blow up. Main reason for that is the fact that all image pixels are treated in a same global way. As previously said, many works were proposed for avoiding this issue (Lerallut *et al.*, 2007; Angulo, 2011; Breuβ *et al.*, 2007). Let us point out the fact that the proposed approach in (Breuβ *et al.*, 2007) is truly adaptive, but is not robust at all, and sophisticated strategies were used to implement the orientation information in the model. In a recent study (Diop and Angulo, 2012b), we overcome those drawbacks by proposing different robust and spatially adaptive PDEs. The first proposed model was a Gaussian regularization of (10), as follow:

$$\partial u_t = \pm\|\nabla u_\sigma\|, \; u(\cdot,0) = I(\cdot) \text{ in } \Omega, \tag{16}$$

where $u_\sigma = u \star G_\sigma$ is the convolution with a Gaussian G_σ of variance σ. This first model solves the robustness against noise; however, it has a major side effect, that is, it creates some blur, and the latter increases as one goes further through scales. This could also

be expected; because, iterating the Gaussian convolution is asymptotically equivalent to solve the Heat equation, which is an isotropic diffusion. Indeed, in a geometrical view, level lines are smoothed both in the normal and tangent directions. We also proposed a second PDE model that behaved in better way than the previous one, as follow (Diop and Angulo, 2012b):

$$\partial u_t = \pm g(\|\nabla u_\sigma\|)\|\nabla u\|, \ u(\cdot, 0) = I(\cdot) \text{ in } \Omega, \tag{17}$$

where g is an edge detector function. In addition to noise robustness, such a model is also locally adaptive to intrinsic image features, *e.g.* edges.

$$g(x) = \begin{cases} 1 + \alpha\|x\|^{2p} \text{ or } 1 + \alpha\exp(\|x\|^{2p}); \ p > 0 & \text{for } g \text{ increasing} \\ \dfrac{1}{1 + \alpha\|x\|^2} & \text{for } g \text{ decreasing}, \end{cases} \tag{18}$$

where $\|\cdot\|$ stands for the euclidean norm in $\mathbb{R}^2$. The monotonicity effects of g will be illustrated later in the numerical results section.

We present in next sections a different and new approach in making robust and adaptive morphological multiscale image analysis methods. In fact, contrary to (Diop and Angulo, 2012b) where the morphological analysis was mainly focused on the processed image, we propose here to work on structuring functions.

Generalized Cauchy problems for continuous multiscale models In order to force both the robustness and adaptability, we propose here[1] a different morphological multiscale approach, by making structuring functions depending on intrinsic image features such as edges. To achieve this, we propose to use the generalized Cauchy problems:

$$\begin{cases} \dfrac{\partial u}{\partial t} = \pm\|Du\|^p \text{ in } \mathbb{R}^N \times (0, T) \\ u(x, 0) = I(x) \text{ on } \mathbb{R}^N \times \{t = 0\} \end{cases} \tag{19}$$

with $p > 1$. The following remark is the starting point of our motivation:

---

[1]The idea was first presented in S⁴G conference (Diop and Angulo, 2012a).

Remark 3.1 *PDE (19) corresponds to multiscale dilations/erosions with:*

– *flat structuring function, for $p = 1$*

– *parabolic structuring function, for $p = 2$.*

Remark 3.1 states also that different kinds of structuring functions can be obtained depending on the value of p. It is then interesting to see how this parameter p behaves when $p \to 1$, $p \in]1, 2[$ and $p \to \infty$, and also how it is linked to the structuring functions in the case of sup-inf formulations. This is in fact done by looking at the viscosity solution of (19), for example with the $+$ sign, which is given (Lions *et al.*, 1987) by Lax-Oleinik formula, as follow:

$$u(x,t) = \sup_{y \in \mathbb{R}^N} \left\{ I(y) - c_p \frac{\|x - y\|^{p/(p-1)}}{t^{1/(p-1)}} \right\}, \text{ where } c_p = \frac{p-1}{p^{p/(p-1)}}. \qquad (20)$$

Let us illustrate some dilations carried out by using equation (20). In fact, we consider an image with ten pixels chosen at random and perform dilations at different scales t and for different p also; results are shown in Figure 1.

For a better comprehension of the effects of p on the structuring function, let us have a closer look for at the family of concave functions $(k_{t,p})_{t>0}$ defined for $t > 0$ and $p > 1$ by:

$$k_{t,p}(x) := -c_p \frac{\|x\|^{p/(p-1)}}{t^{1/(p-1)}}. \qquad (21)$$

First of all, notice that for a fixed $t > 0$, when $p \to 1$, then $k_{t,p} \to 0$; when $p \to \infty$, then for all x, $k_{t,p}(x) \to \|x\|$. What is particularly interesting is to see the behavior of the family of functions $x \to k_{t,p}(x)$ in the unit neighborhood of x; this is illustrated in Figure 2 where different plottings of $k_{t,p}(x)$ are obtained for $t = 1$ and $x \in [-1, 1]$.   Indeed, basically
saying, two facts are shown:

– Firstly, as expected, one is dealing with flat structuring functions as $p \to 1$, on one hand. On the other hand, as p increases up to 2, supports of of structuring functions $k_{t,p}(x)$ diminish and their shapes tend to a parabola (*cf.* Figure 2-(a)).

– Secondly, for $p > 2$, as p increases and $p \to \infty$, shapes of $k_{t,p}(x)$ evolve from a parabola to the limit case, *i.e.* $|x|$ (Figure 2-(b)).

Accounting these two facts and also Remark 3.1, the fundamental idea of our approach is to make p depending on most relevant image features, *i.e.* gradients, which is in fact a nice way to locally adapt structuring functions to intrinsic image features. Thus, we propose two ways in doing that.

Adaptability approach based on image features The basic principle consists in making $p = p(u)$ as a function depending on image gradients, *i.e.* $p = f(\nabla u)$ and $1 < p < \infty$, in a way such that p is close to 1 (around the neighborhood of the considered pixel) in homogeneous image regions, and p belongs to $[2, \infty[$ in inhomogeneous image areas, *e.g.* contours, noise, texture, ... Typical $p = f(\nabla u)$ is given in Figure 3. To this *← insert Fig. 3* end, we propose to set

$$p(u) = 1 + g(\|\nabla u_\sigma\|) \tag{22}$$

in (19)-(20), where g is a decreasing function and given as in (18). Multiscale image analysis results obtained with this approach are shown and discussed previously.

Adaptive coupled model with image features and edge threshold As shown below in the previous section, pretty good results are obtained with the preceding approach. In this section, we wish to significantly increase the robustness against noise. For doing so, we propose to enhance effects of the edge-based parameter $p = p(u) = f(\nabla u)$ by the means of an edge threshold α which determines whether or not one is on image contours.

Let h be a function that detects the image contours. The proposed method is as follows:

– In homogeneous image regions, *i.e.* $h(\|\nabla u\|) < \alpha$, we set

$$p(u) = p_1 = 1 + g_1(\|\nabla u_\sigma\|) \tag{23}$$

in (19)-(20).

– In high frequency image areas, *i.e.* $h(\|\nabla I\|) \geq \alpha$, we set

$$p(u) = p_2 = c + g_2(\|\nabla u_\sigma\|) \tag{24}$$

in (19)-(20), with $c \geq 2$.

For instance, g_1 and g_2 are decreasing edge-based functions taken as in (18), and g_2 is decreasing more rapidly than g_1. Figure 4 illustrates what we just discussed about the edge value α and typical $p(u) = f(\nabla u)$ function used in this work.

NUMERICAL RESULTS

Notation 4.1 *Let us set up the following discretization grid:*

$$x_i = i\triangle x, \; y_j = j\triangle y, \; t^n = n\triangle t$$
$$i, j = 0, \pm 1, \pm 2, \cdots, \; and \; n = 0, 1, 2, \cdots \tag{25}$$

An approximate solution u on the above grid is denoted by $u(x_i, y_j)$, and satisfies:

$$u^n(x_i, y_j) \approx u(i\triangle x, j\triangle y, n\triangle t). \tag{26}$$

Discretization Proposed PDEs (16) and (17) are implemented using an explicit scheme:

$$u^{n+1}(x_i, y_j) = u^n(x_i, y_j) \pm \triangle t \cdot F(u^n(x_i, y_j))(Du^n)_\pm(x_i, y_j), \tag{27}$$

where $F(u^n(x_i, y_j)) \equiv 1$ and $u^n = u^n$ for (10) or $u^n = u^n \star G_\sigma$ for (16), and in the case of dealing with (17), $F(u^n(x_i, y_j))$ corresponds to the discretization of the edge function $g(\|\nabla u_\sigma\|)$. So, the $(+)$ (*resp.* $(-)$) sign in the term $(Du^n)_\pm$ of equation (27) stands for multiscale dilations (*resp.* erosions). It is known that discretization of the hyperbolic term

could be obtained by using (Rouy and Tourin, 1992; Osher and Sethian, 1988). New schemes are also proposed in this work. Before going through that, let us first consider the following forward and backward derivatives:

$$D_x^+ u^n(x_i, y_j) = \frac{u^n(x_i + 1, y_j) - (u^n(x_i, y_j)}{\triangle x},$$

$$D_x^- u^n(x_i, y_j) = \frac{u^n(x_i, y_j) - (u^n(x_i - 1, y_j)}{\triangle x},$$

$$D_y^+ u^n(x_i, y_j) = \frac{u^n(x_i, y_j + 1) - (u^n(x_i, y_j)}{\triangle y},$$

$$D_y^- u^n(x_i, y_j) = \frac{u^n(x_i, y_j) - (u^n(x_i, y_j - 1)}{\triangle y}.$$

Thus, our proposed schemes are the followings:

$$(Du^n)_+ = \sqrt{\max(\max(0, D_x^+ u^n)^2, \max(0, -D_x^- u^n)^2) + \max(\max(0, D_y^+ u^n)^2, \max(0, -D_y^+ u^n)^2},$$
(28)

$$(Du^n)_- = \sqrt{\max(\min(0, D_x^+ u^n)^2, \min(0, -D_x^- u^n)^2) + \max(\min(0, D_y^+ u^n)^2, \min(0, -D_y^+ u^n)^2}.$$
(29)

Note that the discretization of ∇u_σ in $g(\|\nabla u_\sigma\|)$ is not the same as the hyperbolic term. Indeed, we notice that best schemes were obtained by adding all spatial derivatives all together, *i.e.*:

$$\|\nabla u_\sigma^n\|^2 = (D_x^+ u_\sigma^n)^2 + (D_x^- u_\sigma^n)^2 + (D_y^+ u_\sigma^n)^2 + (D_y^- u_\sigma^n)^2.$$
(30)

Results   In this section, we show multiscale image analysis results obtained with the PDE (19) and using either the approach based only on image features or coupled with an edge threshold. The proposed generalized Cauchy-based PDE is solved with suitable numerical schemes like (28) and (29). Other considerations are also accounted; for instance, in the discretization of g, which intervenes in the edge-dependent parameter $p = f(\nabla u)$ in both the feature-based and coupled models.

Obtained results show the efficiency of our locally adaptive approaches for multiscale image analysis. In fact, we first apply such methods on the noisy binary Cat image (Figure 5) obtained by adding a Gaussian noise with an $SNR = 33.29\,db$. Results of the proposed multiscale dilations and erosions are respectively shown in Figures 6 and 7; results are compared to ones carried out by applying the classical PDE-based approach (10). It is not new that pixels are treated in a same global way with (10) which results, as expected again, in a melting between the noise and image features, as one is going through scales (*cf.* first columns from the left in Figures 6 and 7); this fact has been already discussed and illustrated in previous sections. On the contrary, one can see the good behaviors of both the two proposed approaches in the sense of adaptability and robustness against noise, and in an even better manner by using the edge threshold-based technique coupled with image features, as presented before (*cf.* third columns from the left in Figures 6 and 7).

Let us point out another interesting fact regarding the coupled method. In fact, as depicted in Figure 7-(i), one could notice the robustness against noise through scales, and also how the cat whiskers are preserved. By noise robustness, we mean that the noise does not affect at all the performed erosions through scales. To put more emphasis on that fact, we show more erosions in coarser scales in Figure 8. In fact, due to the robustness against noise, thin image features are preserved through scales, which results in a skeletonization of the cat. Thin cat features have high gradients and are then kept similarly to the noise.

Note 4.2 *Skeletal abstraction is a difficult problem that has been greatly studied over years; and obviously it is out of the paper scope. Briefly saying, existing methods for extracting skeletons concern broad research areas comprising topological thinning algorithms (Arcelli and Baja, 1985; Lee and Kashyap, 1994; Borgefors et al., 1999; Bertrand and Couprie, 2009) where Blum grassfire transform (Blum, 1973) were used, curve evolution, variational and wavefront propagation methods (Leymarie and Levine, 1992; Geiger et al., 2003; Tek and Kimia, 2003), Voronoi diagram (Schmitt, 1989; Ogniewicz, 1993; Sheehy et al., 1996), and methods using Euclidean distance function computed*

for example with the Eikonal equation or Hamilton-Jacobi systems (Siddiqi et al., 2002; Torsello and Hancock, 2003; 2004). For more information on that subject, interested readers can have a look on those references.

Proposed methods are applied on the noisy Owl image displayed in Figure 9; multi-scale dilations are erosions are respectively displayed on Figures 10 and 11. Other morphological operations are also performed; namely, openings and closings, and results are displayed in Figure 12 which also confirms good behaviors in terms of noise robustness and locally adaptability of our proposed approaches; especially, the edge threshold-based method presented in the previously section (*cf.* Figures 12-(c) and (f)).

CONCLUSION AND PERSPECTIVES

We provide here some contributions concerning major issues on former morphological operators; for instance, lacks of robustness against noise and adaptability to image features. Our proposed approach is different from what we proposed in (Diop and Angulo, 2012b) in the sense that constraints of robustness and adaptability were not applied anymore on the image itself, but on structuring functions. Also, in this work, we have investigated PDEs for generalized Cauchy problems for modeling robust and adaptive morphological scale-spaces. In addition, the parameter p of the PDE model and the associated sup-inf operators given by Lax-Oleinik formula, have been linked to intrinsic edge image features in two different ways presented in previous sections. As shown by obtained results, the latter approach for choosing p thanks to an edge detector threshold has appeared, as expected, to be extremely robust in a noisy environment. Finally, numerical schemes have also been proposed as well for the resolution of all proposed PDEs. The efficiency of our approaches has been illustrated on synthetic, binary and real images.

As for future work, we plan to extend this study to color, and more generally, to

multichannel images. This is not a straightforward extension of what we have proposed herein, because a channel-wise based approach will undoubtedly result to color artifacts, in the sense that new (artificial) colors that do not primary exist will appear in carried out result. We plan to investigate the channel-wise method, as well as a more challenging vectorial approach, *e.g.* (Bresson and Chan, 2008; Strekalovskiy *et al.*, 2012), even if contexts were different. Finally, it would be interesting to use in edge functions, a time-delay regularization, *e.g.* (Belahmidi and Chambolle, 2005), for avoiding the Gaussian regularization with fixed variances, on one hand, and for locally adaptability too, on another hand.

REFERENCES

Alvarez L, Guichard F, Lions PL, Morel JM (1993). Axioms and Fundamental Equations of Image Processing. Arch Rational Mech Anal 123:199–257.

Alvarez L, Lions PL, Morel JM (1992). Image Selective Smoothing and Edge Detection by Nonlinear Diffusion. ii. SIAM Journal on Numerical Analysis 29:845–66.

Angulo J (2011). Morphological bilateral filtering and spatially-variant adaptive structuring functions. In: ISMM, no. 6671 in LNCS. Italy.

Arcelli C, Baja GSD (1985). A Width-Independent Fast Thinning Algorithm. Transactions on Pattern Analysis and Machine Intelligence PAMI-7:463–74.

Bardi M, Evans LC (1984). On Hopf's formulas for solutions of Hamilton-Jacobi equations. Nonlinear Analysis Theory Methods and Applications 8:1373–81.

Belahmidi A, Chambolle A (2005). Time-delay regularization of anisotropic diffusion and image processing. ESAIM Mathematical Modelling and Numerical Analysis 39:231–51.

Bertrand G, Couprie M (2009). On parallel thinning algorithms: minimal non-simple sets, P-simple points and critical kernels. Journal of Mathematical Imaging and Vision 35:23–35.

Beucher S, Blosseville JM, Lenoir F (1987). Traffic Spatial Measurements Using Video

Image Processing. In: Proceedings of SPIE on Intelligent Robots and Computer Vision, vol. 848. Cambridge, Massachusetts, USA.

Blum H (1973). Biological shape and visual science. Journal of Theoretical Biology 38:205–87.

Borgefors G, Nyström I, Baja GSD (1999). Computing skeletons in three dimensions. Pattern Recognition 32:1225–36.

Bresson X, Chan TF (2008). Fast Dual Minimization of the Vectorial Total Variation Norm and Applications to Color Image Processing. Inverse Problems and Imaging 2:455–184.

Breuβ M, Benedi B, Weickert J (2007). Anisotropic continuous-scale morphology. In: Pattern Recognition and Image Analysis, vol. 4487 of *LNCS*. Berlin, Germany.

Brockett RW, Maragos P (1992). Evolution Equation for Continuous-Scale Morphology. In: IEEE ICASSP. San Francisco, California, USA.

Brockett RW, Maragos P (1994). Evolution Equations for Continuous-Scale Morphological Filtering. IEEE Transactions on Signal Processing 42:3377–386.

Cao F (1998). Partial Differential Equations and Mathematical Morphology. J Math Pures Appl 77:909–41.

Catté F, Dibos F, Koepfler G (1995). A Morphological Scheme for Mean Curvature Motion and Applications to Anisotropic Diffusion and Motion of Level Sets. SIAM J Num Anal 32:1895–909.

Catté F, Lions PL, Morel JM, Coll T (1992). Image Selective Smoothing and Edge Detection by Nonlinear Diffusion. SIAM Journal on Numerical Analysis 29:182–93.

Crandall MG, Ishii H, Lions PL (1992). User's guide to viscosity solutions of second order partial differential equations. Bulletin New Series of The American Mathematical Society 27:1–67.

Cuisenaire O (2006). Locally adaptable mathematical morphology using distance transformations. Pattern Recognition 39:405–16.

Diop EHS, Angulo J (2012a). Morphological scale-spaces image analysis with robust and adaptive pdes. In: International conference on Stereology, Spatial Statistics and Stochastic Geometry. Prague, Czech Republic.

Diop EHS, Angulo J (2012b). Robust Nonlinear PDEs for Multiscale Morphological Image Analysis. In: 83rd Annual Sci. Conf. of Intl' Assoc. of Appl. Math. and Mech. (GAMM). Darmstadt, Germany.

Dorst L, van den Boomgaard R (1994). Morphological Signal Processing and the Slope Transform. Signal Processing 38:79–98.

Geiger D, Liu TL, Kohn RV (2003). Representation and Self-Similarity of Shapes. Transactions on Pattern Analysis and Machine Intelligence 25:86–101.

Grazzini J, Soille P (2009). Edge-preserving smoothing using a similarity measure in adaptive geodesic neighbourhoods. Pattern Recognition 42:2306–16.

Heijmans HJAM (1994). Morphological Image Operators. Boston: Academic Press.

Heijmans HJAM, Ronse C (1990). The Algebraic Basis of Mathematical Morphology - Part I: Dilations and Erosions. CVGIP Image Understanding 50:245–95.

Lee TC, Kashyap RL (1994). Building Skeleton Models via 3-D Medial Surface/Axis Thinning Algorithms. CVGIP Graphical Models and Image Processing 56:462–78.

Lerallut R, Decencière E, Meyer F (2007). Image filtering using morphological amoebas. Image and Vision Computing 25:395–404.

Leymarie F, Levine MD (1992). Simulating the Grassfire Transform Using an Active Contour Model. Transactions on Pattern Analysis and Machine Intelligence 14:56–75.

Lions PL (1982). Generalized solutions of Hamilton-Jacobi equations. London: Pitman Advanced Publishing Program.

Lions PL, Souganidis PE, Vásquez JL (1987). The Relation Between the Porous Medium and the Eikonal Equations in Several Space Dimensions. Revista Matematica Iberoamericana 3:275–340.

Maragos P (1995). Slope Transforms: Theory and Application to Nonlinear Signal Processing. IEEE Transactions on Signal Processing 43:864–77.

Maragos P, Vachier C (2008). A PDE Formulation For Viscous Morphological Operators With Extensions To Intensity-Adaptive Operators. In: IEEE ICIP. San Diego, California.

Maragos P, Vachier C (2009). Overview of Adaptive Morphology: Trends and Perspectives. In: IEEE ICIP. Cairo, Egypt.

Matheron G (1975). Random Sets and Integral Geometry. New York: John Wiley & Sons.

Ogniewicz RL (1993). Discrete Voronoi skeletons. Hartung-Gorre Verlag Konstanz.

Osher S, Sethian JA (1988). Fronts Propagating with Curvature Dependent Speed: Algorithms Based on Hamilton-Jacobi Formulations. Journal of Computational Physics 79:12–49.

Perona P, Malik J (1990). Scale-Space and Edge Detection Using Anisotropic Diffusion. IEEE Transactions on Pattern Analysis and Machine Intelligence 12:629–39.

Rockafellar RT (1970). Convex Analysis. Princeton: Princeton University Press.

Roerdink JBTM (2009). Adaptivity and Group Invariance in Mathematical Morphology. In: IEEE ICIP. Cairo, Egypt.

Rouy E, Tourin A (1992). A viscosity solutions approach to shape-from-shading. SIAM Journal on Numerical Analysis 29:867–84.

Sapiro G, Kimmel R, Shaked D, Kimia BB, Bruckstein AM (1993). Implementing continuous-scale morphology via curve evolution. Pattern Recognition 26:1363–72.

Schmitt M (1989). Some examples of algorithm analysis in computational geometry by means of mathematical morphological techniques. In: Proceedings of the Workshop on Geometry and Robotics, vol. 391. Springer-Verlag.

Serra J (1982). Image Analysis and Mathematical Morphology, vol. I. England: Academic Press.

Serra J (1988). Image Analysis and Mathematical Morphology: Theoretical Advances, vol. II. London: Academic Press.

Sheehy DJ, Armstrong CG, Robinson DJ (1996). Shape Description By Medial Surface Construction. IEEE Transactions on Visualization and Computer Graphics 2:62–72.

Siddiqi K, Bouix S, Tannenbaum A, Zucker SW (2002). Hamilton-Jacobi Skeletons. International Journal of Computer Vision 48:215–31.

Soille P (1999). Morphological Image Analysis. Springer-Verlag.

Sternberg SR (1986). Grayscale morphology. Computer Vision Graphics and Image Processing 35:333–55.

Strekalovskiy E, Chambolle A, Cremers D (2012). A Convex Representation for the Vectorial Mumford-Shah Functional. In: IEEE Conference on Computer Vision and Pattern Recognition (CVPR). Providence, Rhode Island.

Tek H, Kimia BB (2003). Symmetry Maps of Free-Form Curve Segments Via Wave Propagation. International Journal of Computer Vision 54:35–81.

Torsello A, Hancock ER (2003). Curvature Correction of the Hamilton-Jacobi Skeleton. In: IEEE International Conference on Computer Vision and Pattern Recognition.

Torsello A, Hancock ER (2004). A skeletal measure of 2*D* shape similarity. Computer Vision and Image Understanding 95:1–29.

Vachier C, Meyer F (2007). News form viscousland. In: Banon GJF, Barrera J, Braga-Neto UdM, Hirata NST, eds., International Symposium on Mathematical Morphology (ISMM). Rio de Janeiro, Brazil.

van den Boomgaard R, Dorst L (1997). The morphological equivalent of Gaussian scale-space. In: Sporring J, Nielsen M, L. F, Johansen P, eds., Proceedings of Gaussian Scale-Space Theory. Kluwer Academic Publishers.

van den Boomgaard R, Smeulders A (1992). Towards a Morphological Scale-Space Theory. In: O YL, Toet A, Foster D, Heijmans HJAM, Meer P, eds., In Proceedings of the NATO Advanced Research Workshop "Shape in Picure". Springer-Verlag.

van den Boomgaard R, Smeulders A (1994). The Morphological Structures of Images: The Differential Equations of Morphological Scale-Space. IEEE Transactions on Pattern Analysis and Machine Intelligence 16:1101–13.

Verdú-Monedero R, Angulo J, Serra J (2011). Anisotropic Morphological Filters With Spatially-Variant Structuring Elements Based on Image-Dependent Gradient Fields. IEEE Transactions on Image Processing 20:200–12.

(a)

(b)   (c)   (d)
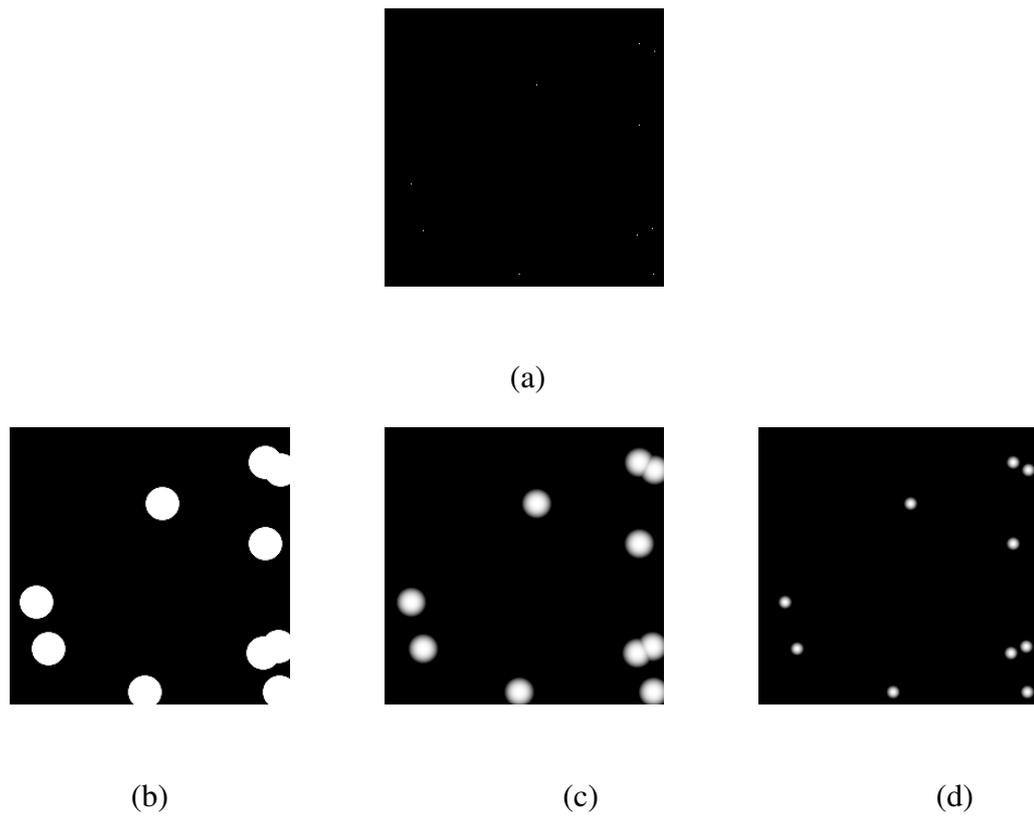
Fig. 1: *(a) Original image with* 10 *pixels chosen at random. Multiscale dilations performed using (20) with (b) $t = 15$ and $p = 1.01$. (c) $t = 20$ and $p = 1.5$. (d) $t = 10$ and $p = 2$.*
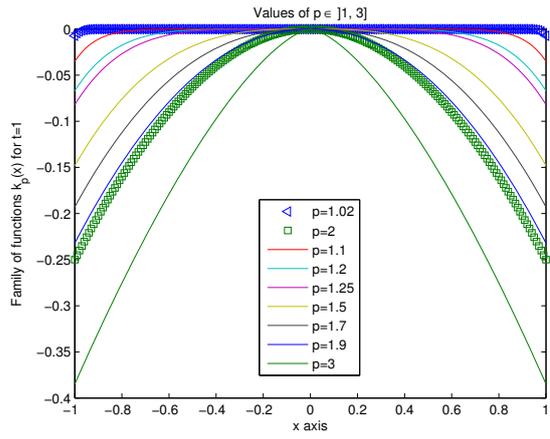
(b)
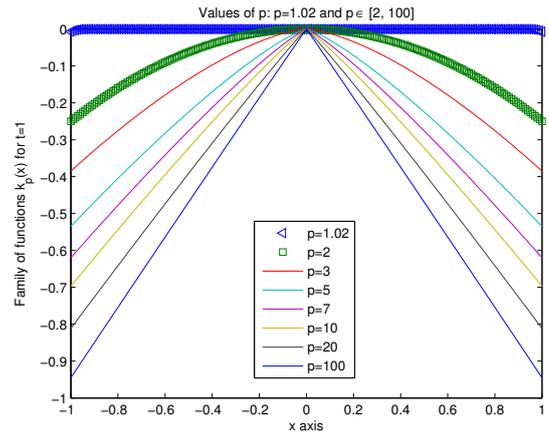
(c)

Fig. 2: *Plottings of $k_{t,p}(x)$ functions for a fixed $t = 1$ and different values of p.*
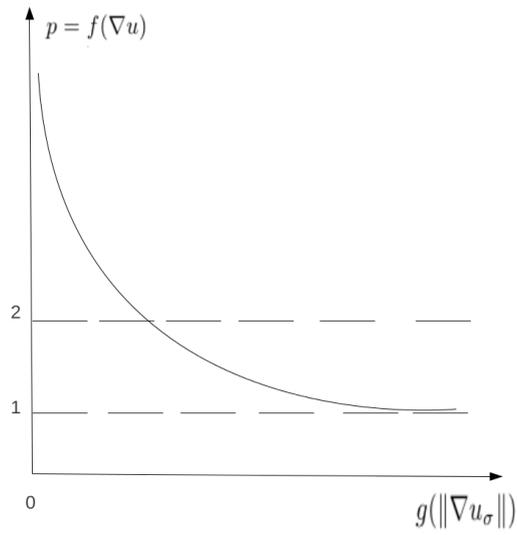
Fig. 3: *Typical $p = f(\nabla u)$ functions for model based on image features.*
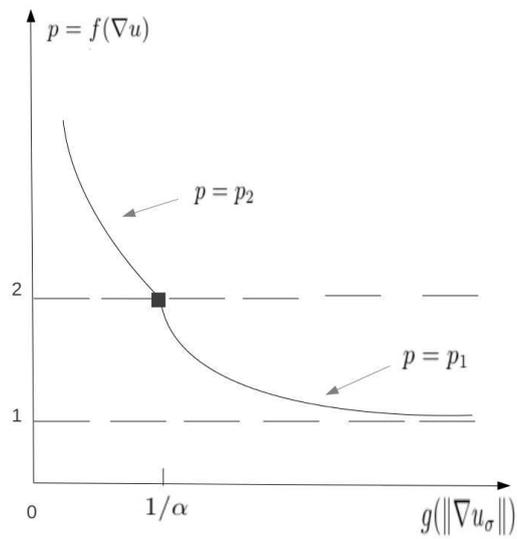
Fig. 4: *Typical $p(u) = f(\nabla u)$ functions for coupled with image features and threshold edge value α.*
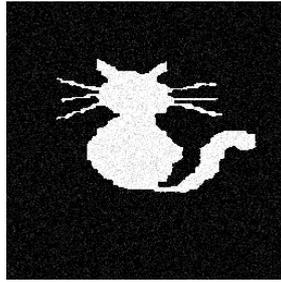
Fig. 5: *Noisy Cat image.*
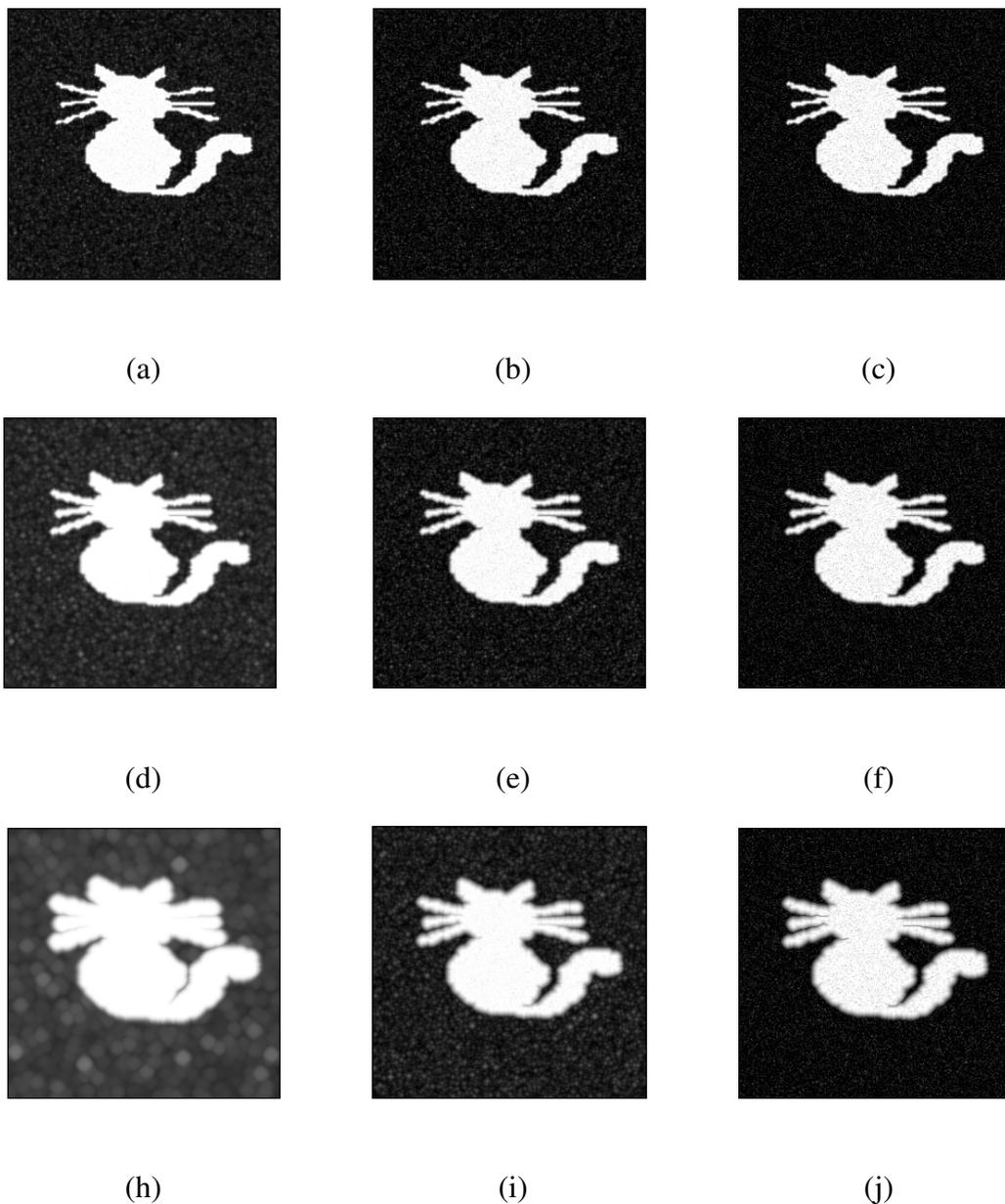
Fig. 6: *Multiscale dilations of the noisy binary Cat image (Fig. 5). From top to bottom −
First line: after 5 iterations using (a) Classical approach (10). Generalized Cauchy based
method (19): (b) p depends only on image features. (c) Coupled edge threshold-based
method. Second line: after 15 iterations using (d) Classical approach (10). Adaptive
PDE (19): (e) p chosen as in precisely section. (f) Edge threshold-based method. Third
line: after 50 iterations using (g) Classical approach (10). Adaptive PDE (19): (h) p
chosen as in previous section. (i) Edge threshold-based method.*
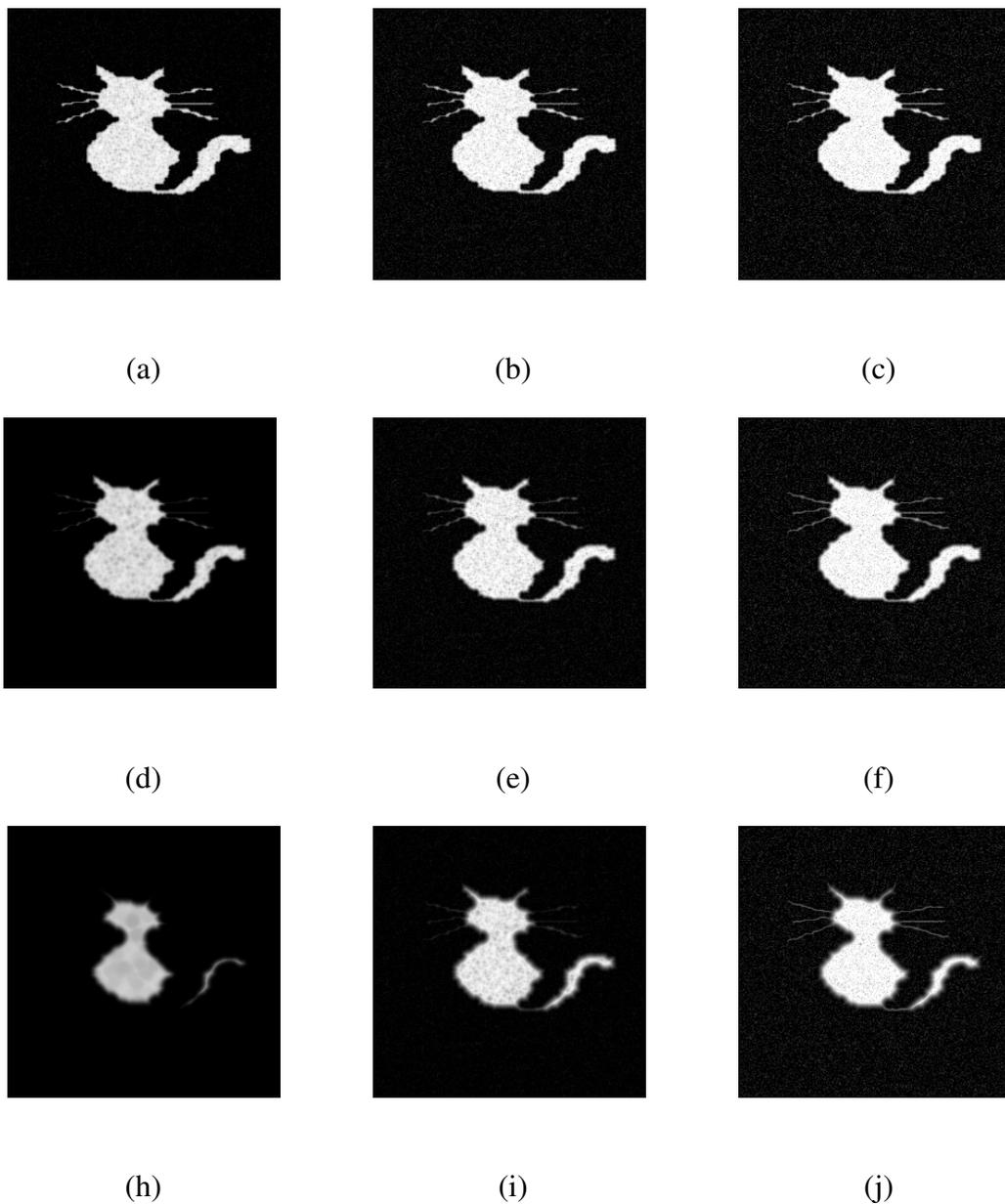
Fig. 7: *Multiscale erosions of the noisy binary Cat image (Fig. 5). From top to bottom −*
First line: after 5 iterations using (a) Classical approach (10). Generalized Cauchy
based method (19): (b) p depends only on image features. (c) Coupled with edge
threshold-based method. Second line: after 15 iterations using (d) Classical approach
(10). Adaptive PDE (19): (e) p chosen as in preceding section. (f) Edge threshold-based
method. Third line: after 50 iterations using (g) Classical approach (10). Adaptive PDE
(19): (h) p chosen as in previous section. (i) Edge threshold-based method.
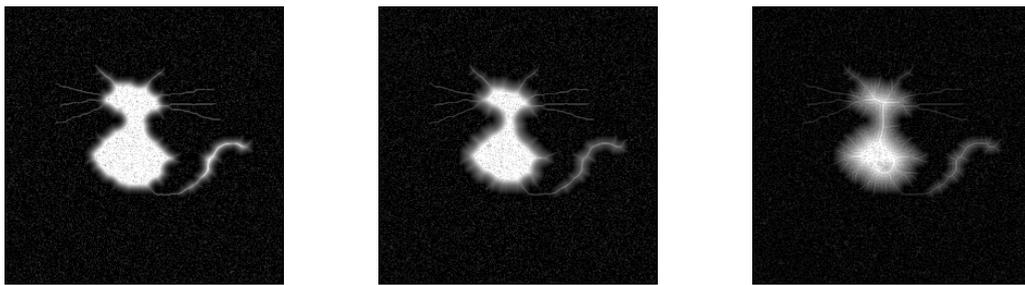
(a) (b) (c)

Fig. 8: *Multiscale erosions of the noisy binary Cat image (Fig. 5) performed with the adaptive PDE (19) coupled with an edge threshold-based method − After: (a)* 100 *iterations. (b)* 200 *iterations and (c) after* 2000 *iterations.*

Fig. 9: *Owl.*

(a) (b) (c)

(d) (e) (f)

(h) (i) (j)
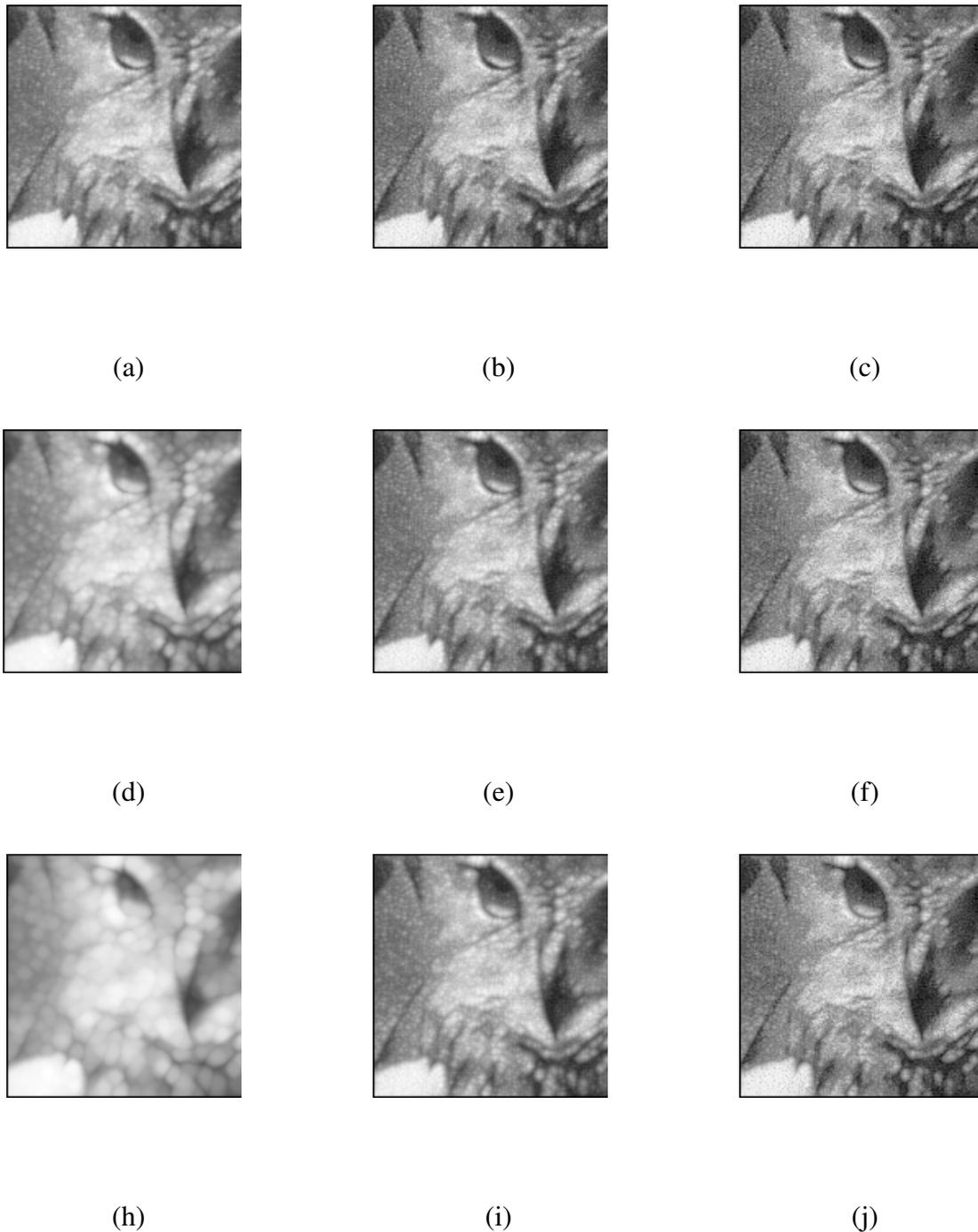
Fig. 10: *Multiscale dilations on noisy Owl image (Fig. 9). From top to bottom − First line: after 5 iterations using (a) Classical approach (10). Generalized Cauchy based method (19): (b) p depends only on image features. (c) Coupled edge threshold-based method. Second line: after 15 iterations using (d) former approach (10). Adaptive PDE (19) (e) p chosen as in previous section. (f) Edge threshold-based method. Third line: after 50 iterations using (g) Classical approach (10). Adaptive PDE (19): (h) p chosen as in previous section. (i) Edge threshold-based method.*
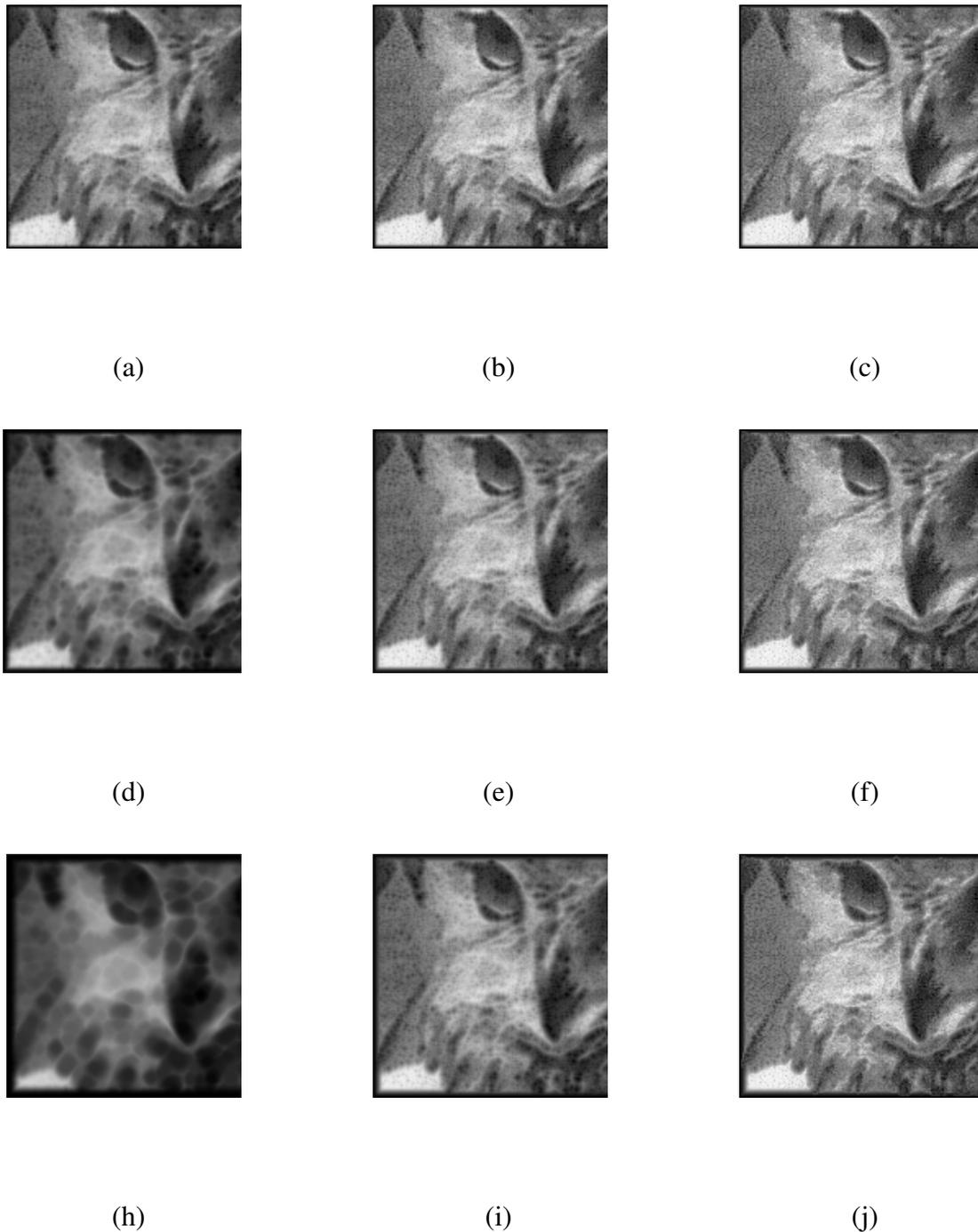
Fig. 11: *Multiscale erosions on noisy Owl image (Fig. 9). From top to bottom − First line: after* 5 *iterations using (a) former approach (10). Generalized Cauchy based method (19):(b) p depends only on image features. (c) Coupled edge threshold-based method. Second line: after* 15 *iterations using (d) former approach (10). (19) (e) p chosen as in preceding section. (f) Edge threshold-based method. Third line: after* 50 *iterations using (g) Classical approach (10). Adaptive (19): (h) p chosen as in previous section. (i) Edge threshold-based method.*

(a) (b) (c)

(d) (e) (f)
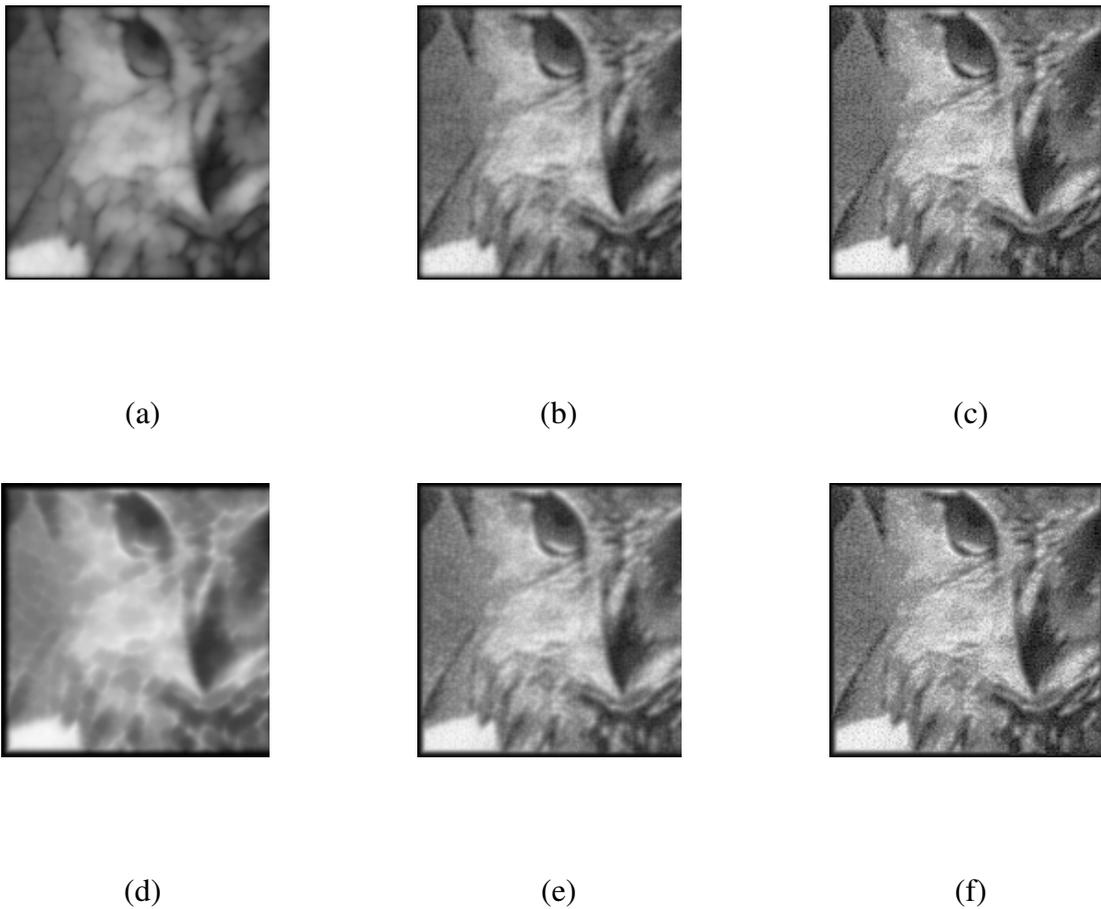
Fig. 12: *Multiscale morphological operations performed on noisy Owl image (Fig. 9). From top to bottom − First line: Multiscale openings at scale* 15 *using: (a) Classical PDE (10). Adaptive PDE (19): (b) p chosen as in preceding section. (c) Edge threshold-based method. Second line: Multiscale closings at scale* 15 *using: (d) Classical PDE (10). Adaptive PDE (19): (e) p chosen as in previous section 3. (f) Edge threshold-based method in preceding section.*